Green Chemistry Letters and Reviews

ISSN: (Print) (Online) Journal homepage: https://www.tandfonline.com/loi/tgcl20

An innovative approach for fatty acid reduction to fatty aldehydes

Jens Johannsen, Gayoung Baek, Georg Fieg & Thomas Waluga

To cite this article: Jens Johannsen, Gayoung Baek, Georg Fieg & Thomas Waluga (2021) An innovative approach for fatty acid reduction to fatty aldehydes, Green Chemistry Letters and Reviews, 14:3, 454-460, DOI: 10.1080/17518253.2021.1943006

To link to this article: https://doi.org/10.1080/17518253.2021.1943006

© 2021 The Author(s). Published by Informa UK Limited, trading as Taylor & Francis Group

Published online: 20 Jun 2021.

Submit your article to this journal

Article views: 156

View related articles

View Crossmark data

Full Terms & Conditions of access and use can be found at
https://www.tandfonline.com/action/journalInformation?journalCode=tgcl20

GREEN CHEMISTRY LETTERS AND REVIEWS
2021, VOL. 14, NO. 3, 454–460
https://doi.org/10.1080/17518253.2021.1943006

Taylor & Francis
Taylor & Francis Group

LETTER

OPEN ACCESS Check for updates

An innovative approach for fatty acid reduction to fatty aldehydes

Jens Johannsen, Gayoung Baek, Georg Fieg and Thomas Waluga

Institute of Process and Plant Engineering, Hamburg University of Technology, Hamburg, Germany

ABSTRACT

The increasing demand for fatty aldehydes as natural flavoring agents nowadays grapples with current production processes requiring harsh reaction conditions and hazardous chemicals. Our research group proved the concept of an innovative, sustainable process based on renewable plant oils for fatty aldehyde production: fatty acids reduction via zerovalent iron. In this study, we present for the first time extensive supporting data characterizing the metal particles used as co-reactants and the core step of the reaction, with varying process parameters. Furthermore, process improvement is demonstrated in that addition of fatty ester-obtained alcohol regenerates metal particles, thereby increasing process yield and selectivity as well as avoiding resource waste. Hexanoic acid reduction to hexanal in the presence of iron particles was used as a reference reaction system, generating a 40% hexanoic acid conversion using Fe 36 µm-particles. To increase overall process sustainability, we explored the possibility of an *in toto* exploitation of the starting materials (esters) through an *a posteriori* reduction of the oxidized iron, exemplarily with the alcohol hexanol. The hexanoic acid conversion rate was thereby increased to 83%, while a 44-fold increase in hexanal yield was observed.

ARTICLE HISTORY
Received 11 May 2020
Accepted 10 June 2021

KEYWORDS
Fatty aldehydes; renewable resources; Green chemistry

Introduction

Flavoring agents, empirically known and used for centuries in the fermentation of food (*1*), make up for a substantial share of the chemical industry market nowadays. Fatty acid esters, fatty acids, fatty alcohols and fatty aldehydes generate over 30 billion USD in revenues worldwide with a 5% yearly growth rate (*2*), mainly supported by the high demand of the developing Asian market and by the American and European quest for 'natural' flavoring agents (3). This call for more sustainable processes is deeply rooted in the global effort to gain independency from fossil starting materials: the synthesis of commercially available fatty aldehydes for example, a fundamental fragrance component for cosmetic use, starts normally from fatty acids derived from petrochemical materials through biochemical *in situ* conversion (4–6).

CONTACT Thomas Waluga thomas.waluga@tuhh.de Institute of Process and Plant Engineering, Hamburg University of Technology, Am Schwarzenberg Campus 4, D-21073 Hamburg, Germany

© 2021 The Author(s). Published by Informa UK Limited, trading as Taylor & Francis Group
This is an Open Access article distributed under the terms of the Creative Commons Attribution License (http://creativecommons.org/licenses/by/4.0/), which permits unrestricted use, distribution, and reproduction in any medium, provided the original work is properly cited.

Not only are fossil raw materials increasingly scarce in our world, but they pose significant challenges in terms of environmental impact: the state of the art technology to chemically synthesize fatty aldehydes requires harsh reaction conditions, namely high temperature – up to 700°C for some products – and pressure values, generating pollution through high energy consumption (7). Therefore, research is focusing on alternative synthesis routes with lower reaction temperatures. However, these alternative routes also depend on the use of hazardous chemicals.

Xie et al. (8) use the toxic component bismuth oxyhalide as a catalyst, acetonitril as solvent and pure oxygen atmosphere for the synthesis of fatty aldehydes from fatty alcohols. Alternatively, metallic organic frameworks (MOF) can be used as catalysts (9): in the 2016 work of Bai et al., the hazardous heterocyclic compound triazine is used as a precursor for the MOF and the synthesis process of the catalyst consumes high amounts of energy. Zheng et al. (10) use hazardous reagents such as dimanganese decacarbonyl and triethylsilane for the synthesis of fatty aldehydes. Also Iosub et al. (11) use silane, as well as the irritant ligand 4,4′-Di-tert-butyl-2,2′-dipyridyl and other hazardous chemicals, for partial reduction of carboxylic acids to aldehydes. Misal et al. (12) describe a method for the synthesis of fatty aldehydes and fatty alcohols from fatty acids: there, the potentially teratogenic solvent toluene is used, or alternatively, the potentially carcinogenic ether tetrahydrofuran in combination with the highly flammable, lung-toxic iron carbonyl as catalyst. Alternative fossilless processes described in literature such as extraction from natural materials or *in vivo* biotransformation through fermenting micro-organisms are extremely time-intensive, call for extensive investment and yield too little final product to cover for the growing demand of the market, thus proving to be industrially and economically inefficient (13–21).

Our review of the state-of-the-art technology for the chemical synthesis of fatty aldehydes, thus, clearly indicates the need for alternative sustainable solutions, starting from renewable educts and avoiding high reaction temperatures as well as the use of hazardous substances.

In this study we present for the first time an innovative, sustainable chemo-enzymatic process for the synthesis of fatty aldehydes from renewable starting materials such as herbal oils, using milder reaction conditions to lower energy consumption and completely avoiding hazardous chemicals. Our process consists of three steps: (1) hydrolysis of the fatty acid ester by a lipase in presence of water, a literature-established reaction that our group previously successfully characterized (22–25), (2) contact of the obtained fatty acid with zerovalent iron particles and finally (3) reduction to the corresponding aldehyde through heating.

The reduction of the fatty acid to fatty aldehyde by reacting with metal particles is the core step of this process: in this paper, we focus on describing and systematically characterizing this reaction under different synthesis conditions, by changing process settings in order to improve aldehyde yield in relation to the available metal atoms. Modified parameters include different metals, different reaction times, different heating rates, and different mass ratios between metal particles and C6-solvents.

In this paper, the exemplary renewable starting material is hexanoic acid, which can be extracted from citrus fruit oils or coconut oil and is liquid, therefore easy to handle (7,26). Its end product hexanal is widely used in detergents, cleaning agents, waxes and as a fragrance in perfumes (7). The final aldehyde yield is evaluated in relation to the molar number of metal atoms available for the reduction reaction: therefore, in this work we present a characterization of the different metal particles, using laser-diffraction Particle Size Distribution (PSD) to calculate volume and surface area of the particles, and Atomic Force Microscopy (AFM) to determine surface roughness. In the following paragraphs, a practical idea for the simultaneous regeneration of the oxidized metal particles is also presented in order to allow for a smaller metal input, thereby increasing sustainability.

An additional plus of this simultaneous regeneration is the possibility of avoiding resource waste, in that when plant oils are used as resource, both their building blocks (fatty acids and alcohols) can be completely consumed during the process.

Materials and methods

In this work, iron and copper particles were used as a zerovalent metal for the reactions. Particle characterization techniques included measuring PSD using a Retsch XT Camsizer, thereby calculating the Sauter diameter of the particles. Additionally, the surface roughness of the iron particles was determined via AFM on a VEECO Dimension 3100 AFM with a Nanoscope IV controller. The number of available metal atoms on the particle surface was then calculated from the known surface area of the metal particles. Table 1 lists the chemicals used in this study.

All experiments were performed in a 100 mL heated batch reactor under a nitrogen atmosphere, in order to prevent oxygen from entering the reactor and oxidizing the metal particles. Experiments performed in triplets proved reproducibility and a maximum error of 7.89% and 17.13% for the conversion calculations, and the yield and selectivity calculations respectively. Samples

Table 1. Chemicals used in this study.

Chemical	Supplier	Product name	Purity [%]	CAS number
Small Fe particles	Laborladen	Iron particles 90 µm	>99	7439-89-6
Large Fe particles	Arteveri	Iron particles 206 µm	>99	7439-89-6
Fe_2O_3	@TEC	Iron-oxide	>99	1309-37-1
Cu	Werth-Metall	Copper	>99	7440-50-8
Hexanal	Alfa Aesar	Hexanal	>98	66-25-1
Hexanol	Alfa Aesar	Hexanol	>99	111-27-3
Hexanoic acid	Sigma-Aldrich	Hexanoic acid	>99	142-62-1

were taken after the experiments and prepared by centrifugation in a Hettich Mikro 120 centrifuge at 13,000 rpm and filtration with a pore diameter of 0.2 µm, in order to remove any solid materials possibly retained in the samples. These were then measured in a PerkinElmer Clarus 500 gas chromatograph with Flame Ionization Detector and nitrogen as the mobile phase. As stationary phase, a 15 m long SLB SUPELCO column with a cross-section area of 0.25 µm × 0.25 µm was used. For sample measurements of the reduction reactions, the oven temperature of the gas chromatograph was set to 130°C for 3.50 min. Then, with a temperature gradient of 30°C/min, the temperature was increased to 160°C. This setting was then held for another 2.50 min. The attenuation for the detection of hexanal was set to −6. Samples of the redox reactions were measured at an oven temperature of 130°C for 2.00 min, then a temperature gradient of 10°C/min was applied until a temperature of 160°C was reached and held for another 2.00 min. The attenuation for the detection of hexanal was set to −5. The Gas chromatography calibration for the reduction reaction experiments was performed with hexanoic acid as a solvent with triplets of at least five concentrations, resulting in a regression coefficient of 0.99. The calibration was performed in the same way for the red-ox reactions, using the educt mixture with the respective educt ratio as solvent.

Results and discussion

Particle characterization

The goal of the particle characterization process is to know the number of iron atoms available for the reaction on the surface of the metal particles. An accurate description of the particles is crucial for an exact calculation of process conversion, yield, and selectivity. Therefore, Sauter diameter, surface roughness, and a precise particle model are necessary.

PSD measurements and calculations according to Equation (1) (27) result in a Sauter diameter of 35.82 µm for the smaller iron particles, and of 74.74 µm for the larger iron particles. These results stand in contrast to the provider's information of a diameter of 90 and 206 µm. An explanation for this deviation lies in the mechanical impact of transport and processing, which may cause grinding and breaking of particles. A Sauter diameter of 19.81 µm emerges from the measurements for copper particles, and a Sauter diameter of 32.15 µm for iron oxide. The surface roughness of the small iron particles resulted in a roughness factor of 1.566, through AFM measurements as shown in Figure 1.

Since these results lie in good agreement with literature data (28,29) for various iron particle sizes, the roughness factor we determined was also used for the calculation of iron surface atoms of the large iron particles.

$$\text{Sauter diameter} = \frac{1}{\sum\left(\frac{\Delta x \times q3}{\bar{x} \times 100}\right)} \tag{1}$$

where $\Delta x$is the size class interval [mm]; $\bar{x}$ is the size class mean value [mm], and $q3$ is the volume density distribution of PSD-measurements

Ten different particle models were then compared to describe particle shapes, resulting in the model of a stellated octahedron as the most suitable. The number of iron atoms on this surface can be geometrically described according to Equation (2), using a lattice constant of 286.65 pm (30). This results in a number of iron atoms of 3.3 µmol/g for Fe 36 µm-particles.

$$N = \frac{A_{metal} \cdot R \cdot 1/L^2}{N_A} \tag{2}$$

where R is the roughness factor; L is the lattice constant [µm] (30); Surface area of the metal [µm^2]; N_A is the Avogadro constant (31) [1/mol].

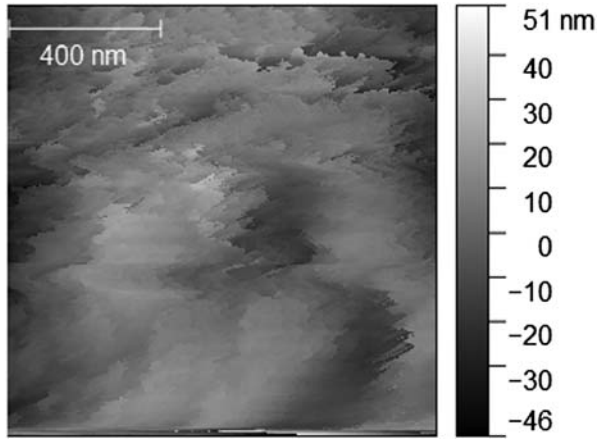

Figure 1. Image obtained from AFM measurements determining a roughness factor of 1.566 for iron.

Table 2. Parameter range for the reduction experiments.

Parameter	Range
Particle	Fe 36 µm Fe 75 µm Cu 20 µm
Mass ratio	0.1–1.5 [$g_{iron}/g_{hexanoic\ acid}$]
Heating rate	13–25 [°C/min]
Reaction time	15–60 [min]

Reduction reaction

Different sets of experiments were performed for the reduction reaction, successively varying the parameters (shown in Table 2) according to the results obtained in the respective previous step in order to find the optimal combination of all available variables, starting with Fe 36 µm-particles. These variables are based on preliminary feasibility studies we completed, to evaluate the possible range of the setting parameters that are physically compatible with the aforementioned experimental setup and methods.

At first, the influence of reaction time on the reduction process was measured using 2 g of Fe 36 µm-particles, with a mass ratio of 0.1 g between iron and hexanoic acid and a heating rate of 13°C/min. As shown in Figure 2, the amount of produced hexanal under the aforementioned process conditions reaches a sharp maximum after 30 min. A longer reaction time leads to more side reactions, and to a decrease in the amount of produced hexanal.

The optimal reaction time of 30 min proves fast in comparison with other synthesis routes for fatty aldehydes. Misal et al. (12) report reaction times of 16–24 h for the reduction of carboxylic acids to toluene using silanes. The Ni-catalyzed reaction reported by Iosub et al. (11) is in the same order of magnitude. Also, Zheng et al. (10) report a reaction time of 3–24 h for aldehyde production through hydrosilylation of carboxylic acids and a subsequent acidic workup using manganese. The photocatalytic oxidation, reported by Xie et al. (8), also takes 24 h.

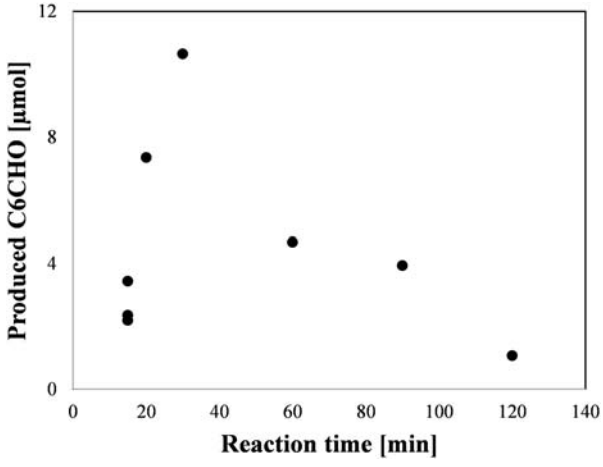

Figure 2. Hexanal production in dependency on the reaction time at a 13 °C/min heating rate and 0.1 mass ratio.

In our work, the highest hexanal amount mirrors a 25% conversion rate of hexanoic acid, with a final yield of 60 $\mu mol_{hexanal}/mol_{hexanoic\ acid}$ and a selectivity of 240 $\mu mol_{hexanal}/mol_{\Delta hexanoic\ acid}$.

Based on these results, parameters were varied according to Table 2. The results of these experiments are seen in Figure 2 and in Table 3; the calculations are based on the reaction shown in Equation (3).

$$3CH_3(CH_2)_4COOH + 2Fe \rightarrow 3CH_3(CH_2)_4CHO + Fe_2O_3 \quad (3)$$

As shown in Table 3, a higher iron mass ratio at the beginning of the reaction leads to an increase in hexanoic acid conversion: this results at the same time in a decrease in selectivity, since more side products are produced. Furthermore, the use of larger iron particles does not benefit hexanal production as can be seen in Exp. #3: the amount of available atoms, in fact, decreases with the increasing particle diameter, due to the decrease of the specific surface area. This indicates the potential to increase production through the use of smaller metal particles. Additionally, as shown by Exp. #7, substituting iron with the alternative base metal copper does not lead to higher hexanal production either. Therefore it can be concluded that copper as a metal is too noble for this reaction. However, our work does not investigate other non-noble metals such as lead or nickel, as their utilization would prove counterproductive to our goal to create a sustainable production process free of hazardous substances. Other research is focusing on solved metals as catalysts (10,12).

The most promising combination of parameters, especially with respect to the critical parameter selectivity, can be found in Exp. #4. Therefore, reaction time and heating rate were varied based on this experiment, resulting in the values shown in Table 4.

As evidenced by the results shown in Table 4, aldehyde selectivity does not improve by varying the two parameters reaction time and heating rate. Higher acid conversions were observed, however, yield and selectivity did not improve. The use of larger iron particles does not lead to a higher hexanal production, confirming the results shown in Table 3.

Therefore, a mass ratio of 0.1 $g_{iron}/g_{hexanoic\ acid}$, a reaction time of 30 min and a heating rate of 25°C, as indicated by Exp. #4 (Table 3), make up the most promising combination for further investigations. The obtained yield of 70 µmol/mol is quite low in

Table 3. Parameters and experimental results of the reduction reaction (Exp #0–Exp #7).

Parameter	Exp. #0	Exp. #1	Exp. #2	Exp. #3	Exp. #4	Exp. #5	Exp. #6	Exp. #7
Particles	36µ-Fe	36µ-Fe	36µ-Fe	75µ-Fe	36µ-Fe	36µ-Fe	36µ-Fe	20µ-Cu
Mass ratio [g/g]	0.1	0.1	0.1	0.1	0.1	1.0	1.5	0.1
Heating rate [°C/min]	13	13	13	13	25	13	13	13
Reaction Time [min]	30	15	60	30	30	30	30	30
Conversion [%]	26	15	33	35	29	61	70	3
Yield [µmol/mol]	60	20	30	20	70	130	12	1
Selectivity [µmol/mol]	240	130	80	50	240	210	18	20

Table 4. Parameters and experimental results of the reduction reaction (Exp #8–Exp #10).

Parameter	Exp. #8	Exp. #9	Exp. #10
Particles	36µ-Fe	75µ-Fe	36µ-Fe
Mass ratio [g/g]	0.1	0.1	0.1
Heating rate [°C/min]	25	25	13
Reaction Time [min]	60	30	30
Conversion [%]	40	39	25
Yield [µmol/mol]	90	20	60
Selectivity [µmol/mol]	220	60	240

comparison to the results of other synthesis routes (8–12) due to the limited number of available iron atoms. Therefore, in this work, a strategy was developed to regenerate the iron atoms *in situ*.

Red-ox reaction

After successfully producing hexanal from hexanoic acid through a one-way reduction reaction, the goal of increasing aldehyde production was pursued by adding an alcohol to reduce the oxidized metal. In the overall process, the alcohols produced by the hydrolysis of fatty esters (first step according to (25)) could realize this reduction, thus enhancing productivity in the subsequent aldehyde production step. As proof of concept, hexanol was added to the experiments in addition to hexanoic acid: the alcohol gets in turn oxidized, thus forming additional hexanal.

Three different metal particles were chosen as co-reactants for the following experiments: Fe 36 µm-particles, Fe 75 µm-particles, and Fe_2O_3 particles (thereby starting with the oxidized iron form). Experimental settings such as a heating rate of 25°C/min and a reaction time of 30 min were chosen in accordance with the best set of parameters emerged from the reduction reaction experiments displayed in the previous paragraph. The overall parameter range for the experiments conducted as red-ox reactions are shown in Table 5. The results of experiments 11–14 can be seen in Table 6.

Table 5. Parameter range for the red-ox reaction experiments.

Parameter	Range
Particle	Fe 36 µm
	Fe 75 µm
	Fe_2O_3 32 µm
Mass ratio	0.1 [$g_{hexanol}/g_{educt}$]
Educt ratio	1–2 [$g_{hexanol}/g_{hexanoic\ acid}$]
Heating rate	25 [°C/min]
Reaction time	30 [min]

As a starting point for the series shown in Table 6 (Exp. #11–Exp #13, Table 6), an educt ratio of hexanoic acid/hexanol of 1:1 was chosen, as this represents the idea of the complete process: vegetable oils serving as resources are in fact esters, containing one alcohol per fatty acid.

As evidenced by this set of data shown in Table 6, hexanal yield and selectivity increased by two orders of magnitude, proving alcohol addition beneficial for the process. The experiments with Fe 36 µm-particles show the highest yield and selectivity with respect to both the acid (8 $mmol_{hexanal}/mol_{\Delta hexanoic\ acid}$) and the alcohol (42 $mmol_{hexanal}/mol_{\Delta hexanol}$). This particle size was therefore chosen for further investigation. Varying the ratio of the educts by adding external alcohol at the beginning of the reaction results in a more than 16% increase in acid conversion, and a six-fold and 4.5-fold increase of hexanal yield and hexanal selectivity respectively, with respect to hexanoic acid (Exp. #14, Table 6). With respect to hexanol, hexanal yield and selectivity increased even more significantly, reaching values of 13 $mmol_{hexanal}/mol_{hexanol}$ and 1190 $mmol_{hexanal}/mol_{\Delta hexanol}$ respectively. Conclusively, Fe 36 µm-particles at a mass ratio of 0.1 g_{iron}/g_{educt}, and a heating rate of 25°C/min for a reaction time of 30 min resulted in the most effective hexanal production, indicating possible trends for further yield improvement. Adding external alcohol proved to be a promising approach for process improvement,

Table 6. Parameters and experimental results of the redox reaction (Exp #11–Exp #14).

Parameter Particles	Exp. #11 36µ-Fe	Exp. #12 75µ-Fe	Exp. #13 32µ-Fe2O3	Exp. #14 36µ-Fe
Mass ratio [g/g]	0.1	0.1	0.1	0.1
Educt ratio [g/g]	1	1	1	2
Heating rate [°C/min]	25	25	25	25
Reaction Time [min]	30	30	30	30
$Conversion_{acid}$ [%]	71	77	65	83
Yield [$mmol/mol_{acid}$]	5	2	1	30
Selectivity [$mmol/mol_{acid}$]	8	3	2	36
ConversionAlcohol [%]	11	36	11	110
Yield [$mmol/mol_{alcohol}$]	5	2	1	13
Selectivity [$mmol/mol_{alcohol}$]	42	5	10	1190

ending up with a yield of 3% in respect to hexanoic acid alone. Misal et al. (12) have reported aldehyde yields from 1% to 98%, depending on type of solvent (either toluene or tetrahydrofuran), type of silane and type of iron carbonyl. Xie et al. (8) have reported yields from 1.6% to 91.1%, depending on the catalyst (either BiOCl or BiOBr) and on the reaction atmosphere (O_2 or N_2). Iosub et al. (11) have reported yields from 3% to 96% depending on reaction conditions (different mixtures of hazardous solvents and Ni-complexes).

Conclusion and outlook

The aim of this work is to systematically characterize the crucial fatty acid reduction step of our process for sustainably synthesizing fatty aldehydes from renewable resources using zerovalent iron at comparably low temperatures and in the absence of hazardous chemicals. Archetypal for our efforts is the reduction of hexanoic acid to hexanal, a compound widely used for cosmetic and cleansing purposes.

The prerequisite for reaction characterization is the number of metal atoms available for it on the metal particles used as co-reactants. This in turn requires accurate metal particle characterization, which we present in this work for different metals.

Suitable operating starting points for our characterization were found by successfully carrying out the reduction reaction: for Fe 36 µm-particles with a mass ratio of 0.1 $g_{iron}/g_{hexanoic\ acid}$, a reaction time of 30 min and a heating rate of 25°C/min proved the most promising, generating a 40% hexanoic acid conversion.

To increase overall process sustainability, we explored the possibility of *in toto* exploitation of the starting materials through an *a posteriori* reduction of the oxidized iron: the alcohol hexanol was thus added as proof of concept. Once again, Fe 36 µm-particles showed the most favorable conversion rates: with an educt ratio of 1 g/g, a hexanoic acid conversion of 71% was achieved. Adding excess alcohol further increased hexanoic acid conversion to 83%.

In contrast to other reported synthesis routes, the selectivity of this process poses a challenge. However, the selectivity values demonstrated in the red-ox step, all the while waiving harsh reaction conditions and hazardous chemical catalysts, are a good basis for further research and constitute an additional layer of sustainability in our process, allowing the unfolding of its full ecological potential. The findings presented in this paper lay the groundwork for larger-scope development of this concept, building on our laboratory-scale results to implement an energy-sparing, holistically green and economically remunerative process for the industrial production of fatty aldehydes. For further research, a model-based approach has to be favored in order to adequately describe the process from a mathematical point of view, thus laying the basis for a structured process improvement (5,32) to increase yield. While process improvement will focus on increasing fatty aldehyde yield, further investigations of the trade-off between avoiding hazardous chemicals and achieving higher production yields should be performed. Thereby, a life-cycle assessment can evaluate the ecological benefits of the different fatty aldehyde synthesis routes, weighing the ecological factor against process yield and selectivity.

Notation

A_{metal}	surface area of the metal [µm^2]
AFM	atomic force microscopy
Cu	copper
Fe	iron
L	lattice constant [µm]
MOF	metallic organic frameworks
N	number of atoms on surface [mol]
N_A	Avogadro constant [mol^{-1}]
PSD	particle size distribution

Acknowledgements

The authors would like to thank the Institute of Solids Process Engineering and Particle Technology of TUHH in the person of Lennard Lindmüller and the Institute of Materials Physics and Technology of TUHH in the person of Manuel Brinker for their support in the metal particles characterization, and Dr Valentina Scita for accurately proofreading the manuscript.

Disclosure statement

No potential conflict of interest was reported by the author(s).

Funding

This work was supported by Free and Hanseatic City of Hamburg [grant number LFF-FV43].

ORCID

Jens Johannsen http://orcid.org/0000-0002-8159-890X
Thomas Waluga http://orcid.org/0000-0001-5308-3338

References

[1] Belitz, H.-D.; Grosch, W.; Schieberle, P. *Food Chemistry, 3rd rev. ed. / H.-D. Belitz, W. Grosch, P. Schieberle Translation from the Fifth German Edition by M.M. Burghagen*; Springer: Berlin, 2004.
[2] IAL Consultants. *An Overview of the Global Flavors & Fragrances Market, 11th ed.*: IAL Consultants: London, 2018.
[3] Balagiannis, D. P. Predicting Aroma Formation with Kinetic Models. In *Flavour Development, Analysis and Perception in*

Food and Beverages; Parker, J.K., Elmore, J.S., Methven, L., Eds.; Elsevier: Cambridge, 2015; pp 211–233.
[4] Sánchez, M.A.; Torres, G.C.; Mazzieri, V.A.; Pieck, C.L. Selective Hydrogenation of Fatty Acids and Methyl Esters of Fatty Acids to Obtain Fatty Alcohols-a Review. *J. Chem. Technol. Biotechnol.* **2017**, *92* (1), 27–42.
[5] Yenumala, S.R.; Maity, S.K.; Shee, D. Reaction Mechanism and Kinetic Modeling for the Hydrodeoxygenation of Triglycerides Over Alumina Supported Nickel Catalyst. *React. Kinet., Mech. Catal.* **2017,** *120* (1), 109–128.
[6] Chen, Y.-Z.; Wang, Z.U.; Wang, H.; Lu, J.; Yu, S.-H.; Jiang, H.-L. Singlet Oxygen-engaged Selective Photo-oxidation Over Pt Nanocrystals/Porphyrinic MOF: The Roles of Photothermal Effect and Pt Electronic State. *J. Am. Chem. Soc.* **2017**, *139* (5), 2035–2044.
[7] *Ullmann's Encyclopedia of Industrial Chemistry*; Wiley-VCH Verlag GmbH & Co. KGaA: Weinheim, 2000.
[8] Xie, F.; Zhang, Y.; He, X.; Li, H.; Qiu, X.; Zhou, W.; Huo, S.; Tang, Z. First Achieving Highly Selective Oxidation of Aliphatic Alcohols to Aldehydes Over Photocatalysts. *J. Mater. Chem. A* **2018**, *6* (27), 13236–13243.
[9] Bai, C.; Li, A.; Yao, X.; Liu, H.; Li, Y. Efficient and Selective Aerobic Oxidation of Alcohols Catalysed by MOF-Derived Co Catalysts. *Green Chem.* **2016,** *18* (4), 1061–1069.
[10] Zheng, J.; Chevance, S.; Darcel, C.; Sortais, J.-B. Selective Reduction of Carboxylic Acids to Aldehydes Through Manganese Catalysed Hydrosilylation. *Chem. Commun.* **2013**, *49* (85), 10010–10012.
[11] Iosub, A.V.; Moravčík, Š; Wallentin, C.-J.; Bergman, J. Nickel-Catalyzed Selective Reduction of Carboxylic Acids to Aldehydes. *Org. Lett.* **2019,** *21* (19), 7804–7808.
[12] Misal Castro, L.C.; Li, H.; Sortais, J.-B.; Darcel, C. Selective Switchable Iron-Catalyzed Hydrosilylation of Carboxylic Acids. *Chem. Commun.* **2012**, *48* (85), 10514–10516.
[13] Gallage Nethaji J., Hansen Esben H., Kannangara Rubini, Olsen Carl Erik, Motawia Mohammed Saddik, Jørgensen Kirsten, Holme Inger, Hebelstrup Kim, Grisoni Michel, Møller Birger Lindberg Vanillin Formation from Ferulic Acid in Vanilla Planifolia is Catalysed by a Single Enzyme. *Nat. Commun.* **2014,** *5*, 4037.
[14] Chouchi, D.; Barth, D.; Reverchon, E.; Della Porta, G. Bigarade Peel Oil Fractionation by Supercritical Carbon Dioxide Desorption. *J. Agric. Food Chem.* **1996,** *44* (4), 1100–1104.
[15] Palma, M.; Taylor, L.T.; Varela, R.M.; Cutler, S.J.; Cutler, H.G. Fractional Extraction of Compounds from Grape Seeds by Supercritical Fluid Extraction and Analysis for Antimicrobial and Agrochemical Activities. *J. Agric. Food Chem.* **1999,** *47* (12), 5044–5048.
[16] Braga, A.; Guerreiro, C.; Belo, I. Generation of Flavors and Fragrances Through Biotransformation and De Novo Synthesis. *Food Bioprocess Technol.* **2018,** *11* (12), 2217–2228.
[17] Hu, Z.; Greenfield, D.; Arlagadda, V. 2012. Methods and Compositions for Enhanced Production of Fatty Aldehydes and Fattyl Alcohols. 13/359,127, Jan 26, 2012.
[18] Fleige Christian, Meyer Florian, Steinbüchel Alexander, Liu S.-J. Metabolic Engineering of the Actinomycete *Amycolatopsis* sp. Strain ATCC 39116 Towards Enhanced Production of Natural Vanillin. *Appl. Environ. Microbiol.* **2016,** *82* (11), 3410–3419.
[19] Sinha, A.K.; Sharma, U.K.; Sharma, N. A Comprehensive Review on Vanilla Flavor: Extraction, Isolation and Quantification of Vanillin and Others Constituents. *Int. J. Food Sci. Nutr.* **2008,** *59* (4), 299–326.
[20] Schmid, R.D. *Taschenatlas der Biotechnologie und Gentechnik, Dritte Auflage*; Wiley-VCH: Weinheim, 2016.
[21] Wittmann, C.; Liao, J.C. *Industrial Biotechnology: Products and Processes*; Wiley-VCH Verlag GmbH & Co. KGaA: Weinheim, 2018.
[22] Krause, P.; Fieg, G.; Zeng, A.-P. *Modellierung und kombinierte experiment- und simulationsbasierte Analyse eines zweiphasig durchströmten enzymatischen Festbettreaktors*; Shaker: Aachen, 2013.
[23] Leipold, M. *Ganzheitliche Analyse enzymkatalytischer Syntheseprozesse im Festbettreaktor*; Shaker: Aachen, 2014.
[24] Ajmal, M.; Fieg, G.; Keil, F. Analysis of Process Intensification in Enzyme Catalyzed Reactions Using Ultrasound. *Chem. Eng. Process.* **2016,** *110*, 106–113.
[25] Johannsen, J.; Meyer, F.; Fieg, G.; Waluga, T. Process for the Preparation of Fatty Aldehydes from Renewable Resources. *Chem. Ing. Tech.* **2020,** *92* (6), 777–781.
[26] Hagen, J.; Henke, D.-I.D. Katalysatorscreening bei der Umesterung von Fetten und Ölen mit Ethanol. *Chem. Ing. Tech.* **2009,** *81* (9), 1429–1438.
[27] Draxler, J.; Siebenhofer, M. Partikelgrößen und Partikelgrößenverteilungen. In *Verfahrenstechnik in Beispielen*; Draxler, J., Siebenhofer, M., Eds.; Springer Fachmedien Wiesbaden: Wiesbaden, 2014; pp 239–258.
[28] Fujii, Y.; Nakayama, T.; Yoshida, K. Roughness Estimation of Polycrystalline Iron Surface Under High Temperature by Small Glancing Angle X-ray Scattering. *ISIJ Int.* **2004,** *44* (9), 1549–1553.
[29] Kleber, C.; Weissenrieder, J.; Schreiner, M.; Leygraf, C. Comparison of the Early Stages of Corrosion of Copper and Iron Investigated by in situ TM-AFM. *Appl. Surf. Sci.* **2002,** *193* (1-4), 245–253.
[30] Seki, I.; Nagata, K. Lattice Constant of Iron and Austenite Including Its Supersaturation Phase of Carbon. *ISIJ Int.* **2005,** *45* (12), 1789–1794.
[31] Bureau International des Poids et Mesures. 2020. Resolution 1 of the 26th CGPM. https://www.bipm.org/en/CGPM/db/26/1/ (accessed October 7, 2020).
[32] Otsuki, A.; Pereira Gonçalves, P.; Leroy, E. Selective Milling and Elemental Assay of Printed Circuit Board Particles for Their Recycling Purpose. *Metals. (Basel)* **2019,** *9* (8), 899.